ELSEVIER

International Journal of Solids and Structures 41 (2004) 3293–3316

INTERNATIONAL JOURNAL OF SOLIDS and STRUCTURES

www.elsevier.com/locate/ijsolstr

Softening behavior of reinforced concrete beams under cyclic loading

Sonia Marfia *, Zila Rinaldi, Elio Sacco

Dipartimento di Meccanica, Strutture, A&T Università di Cassino, Via G. Di Biasio 43, 03043 Cassino, Italy

Received 13 February 2003; received in revised form 2 December 2003

Available online 27 February 2004

Abstract

Aim of the paper is the study of the cyclic behavior of reinforced concrete beams taking into account the compression and tensile softening in the concrete material, the Baushinger effect in the steel and an adequate bond-slip law for the concrete–steel interface. Nonlinear material models are developed on the basis of damage mechanics and plasticity. In particular, an elastoplastic-damage model is developed for the concrete material introducing two damage variables, one in tension and one in compression. A plasticity model with nonlinear hardening is adopted for the reinforcing steel and a bond stress–slip law, suitable for cyclic behavior, is introduced for the concrete–steel interface.

The governing equations are derived and a numerical procedure based on the arc-length method, within an implicit Euler algorithm for the time integration, is developed.

Some numerical examples are carried out in order to analyze the axial and bending behavior of reinforced concrete beams under monotonic and cyclic loading. A comparison with experimental results available in literature is performed in order to validate the proposed model.

Keywords: Reinforced concrete beams; Damage; Plasticity; Bond-slip law; Cyclic behavior; Numerical procedures

1. Introduction

One-dimensional cementitious structural elements such as beams and arches are widely used in civil engineering constructions. Classical textbooks, e.g. (Park and Paulay, 1975), present deep studies on the behavior and modeling of reinforced concrete beams; thus, detailed descriptions of structural design of concrete beams reinforced by classical steel bars are given.

Although many studies have been already developed in the topic of modeling of the mechanical behavior of reinforced concrete constructions, the research in this field is still very active due to the complexity arising from the composite nature of this material. Structural reinforced concrete, in fact, presents a nonlinear behavior governed by different phenomena related to the nonlinear constitutive laws of the

* Corresponding author. Tel.: +39-776-2993745; fax: +39-776-2993392.
E-mail address: marfia@unicas.it (S. Marfia).

0020-7683/$ - see front matter © 2003 Elsevier Ltd. All rights reserved.
doi:10.1016/j.ijsolstr.2003.12.015

materials, and to the bond behavior between them. Even if simplified methodology can be adopted, particularly for strength definition, an accurate prediction of cracking and deflections of reinforced concrete structures under working loads, and the assessment of the safety of structures against failure, cannot neglect the analysis of tension stiffening, concrete softening, slip at the steel-concrete interface and crushing. Furthermore the presence of cyclic loading, typical of seismic actions, introduces other problems related to stiffness degradation in concrete, Bauschinger effect in reinforcing steel, and bond degradation between concrete and reinforcement.

The behavior of reinforced concrete depends on the combined action of the concrete and its embedded reinforcement. This composite action is produced by the bond stress at the interface of the two materials. The crucial point of the study of the mechanical behavior of cementitious structures is the definition of proper constitutive laws and of a suitable model, able to reproduce the structural response of reinforced concrete elements. Cementitious materials are characterized by a softening response with different strength in compression and in tension. In particular, experimental results show that these materials present brittle behavior in tension and inelastic deformations accompanied by damage effects in compression.

On the basis of experimental evidences, different authors have proposed simplified stress–strain relationships for concrete in compression, also taking account of the confinement effect produced by the stirrups. Starting from one of the first models proposed by Chan (1955), which described the nonlinear behavior of compressed concrete by a trilinear curve, many authors improved the modeling of the concrete behavior, considering nonlinear softening branches (Kent and Park, 1971; Sargin et al., 1971).

Furthermore, the concrete presents softening behavior both in compression and tension, giving rise to localization effects in reinforced concrete structures. The compressive damage zone (CDZ) model was developed by Markeset (1993) to study the failure of concrete under compression, taking account of the presence of a localized damage near a crack.

The definition of the tensile behavior of concrete and, in particular, of the so-called tensile softening behavior is of paramount importance, as this last aspect controls the transition modality from the undamaged stage to the cracked one. In fact, the tensile brittle behavior of the concrete gives rise to cracking phenomena in the structure.

The mechanical behavior of cementitious materials have been modeled using concepts of the fracture mechanics, or of the continuum damage mechanics neglecting or considering the plasticity effects. The fictitious crack model (FCM) was developed by Hillerborg (1983) to characterize the fracture of concrete in tension. The model is based on the principle that the deformation, in the post-peak range, is localized in a damage zone (fracture process zone).

In the framework of continuum damage mechanics, different models, which account not only for the damage effects but also for the inelastic, i.e. plastic, deformations have been proposed in literature. Among the models which take into account both the damage and the plastic behavior, Abu-Lebdeh and Voyiadjis (1993) formulated a plastic-damage model for concrete under cyclic loading, adopting a bounding surface concept. Luccioni et al. (1996) proposed a thermodynamically consistent plastic and damage model, based on the classical plasticity theory and isotropic damage theory. Borino et al. (1996) developed a thermodynamically consistent elastoplastic-damage model, which considers the coupling between the plasticity and damage internal variables. Carol and Bažant (1997) considered the damage and plasticity effects into the framework of the microplane theory. Meschke et al. (1998) proposed a model for plain concrete based on the multisurface elastoplastic-damage theory. In that paper anisotropic stiffness degradation and inelastic deformations are taken into account. de Borst et al. (1999) developed constitutive plastic-damage models combining gradient plasticity with scalar damage and gradient damage with isotropic plasticity. Addessi et al. (2001) presented a nonlocal elastoplastic-damage model for cementitious materials, considering the damage evolution in compression depending on the total deformation.

The analysis of simple elements, therefore, cannot neglect the softening response in tension and in compression of the concrete due to the damage and inelastic deformations occurring in the material.

Between two subsequent cracks, in fact, tensile stresses are transmitted from the steel to the concrete by means of bond actions; stress and strain redistributions occur along the structural elements and the concrete contributes to support tensile strength and to increase the stiffness of the element, giving rise to the so-called tension stiffening effects. In these zones the strain in the reinforcement is reduced depending on the spacing of the cracks and the bond characteristics of the rebar.

The full compatibility between concrete and reinforcement strains can be assumed only for low strain levels. When the load level is increased, particularly in the surrounding of the cracks, high slips develop, causing relative displacements between the concrete and the reinforcement steel.

The fundamental role of the interaction between reinforcing steel and surrounding concrete through bond-slip is particularly remarkable in the cyclic behavior of reinforced concrete structures, when bond deterioration can occur due to the damage caused by the load reversals. The definition of a suitable bond-slip law is a wide discussed problem, and even if a great number of works deals with this topic, a finite assessment is still not reached (CEB-FIP Bulletin, 2000).

The first studies date back to sixties. Rehm (1961) showed the existence of a slip between the steel rebar and concrete and the related bond actions. Ngo and Scordelis (1967) developed a bond-slip model in the framework of a finite element analysis by means of bond link elements introduced between concrete and steel. Starting from these studies, on the basis of experimental and numerical results, different relationships between bond stress and slip have been proposed (Ciampi et al., 1981; Harajli et al., 1995; Gambarova and Rosati, 1996; Bigaj, 1999). In particular, the steel–concrete interface model reported in CEB-FIP Model Code (1990) is based on the theory developed by Eligehausen et al. (1983).

The first analytical model for reversed cyclic bond behavior was proposed by Morita and Kaku (1973). The model, considered not sufficiently accurate for several load cycles and for large slip values, was improved in the 1980s by Tassios and Yannopoulos (1981) and Filippou et al. (1983). A more refined model was proposed by Balàzs (1991), defining a reversed cyclic envelop with reductions of the bond strength.

Experimental analyses to establish the relationship between bond stress, steel stress and slip were carried out by Kankam (1997). The variation of the steel strain along the length of embedded bars, anchored at the midpoint, was directly measured by the authors by means of tests conducted on double pullout specimens. The obtained results, related to elastic behavior of the steel reinforcement, provide the basis for the calculation of bond stress variation and local slip along the embedded length and for the definition of relationships between bond stress, steel stress and slip. Numerical solutions of the bond-slip problem, related also to cyclic loads, were proposed by Ayoub and Filippou (1999).

The evaluation of the local behavior of a reinforced concrete element, taking account of the above described phenomena, is a difficult task and it requires accurate modeling of the materials. The definition of a moment–mean curvature relationship, that simulates the behavior of the whole cracked element, was proposed by Grimaldi and Rinaldi (2000) in the case of monotonic loads and by Kwak and Kim (2001) in case of cyclic loads.

Numerical solutions have been proposed by different authors. A fiber beam element accounted for the bond-slip was formulated by Monti and Spacone (2000), cyclic behavior of reinforced concrete beam-column elements were studied by finite elements analyses by Kwan and Billington (2001).

Aim of the present paper is the definition and evaluation of a suitable approach for predicting the cyclic behavior of reinforced concrete structural elements. Nonlinear material models are defined on the basis of damage mechanics and plasticity. Compression and tension strain-softening, Bauschinger effect, and adequate bond-slip law are accounted for.

In particular, a one-dimensional model for a beam element of reinforced concrete is proposed. A thermodynamically consistent elastoplastic-damage model is developed for the concrete material introducing two damage variables, one in tension and one in compression, accounting for the crack closure unilateral phenomenon. The damage evolution is governed by the elastic strain as the experimental evidences show. A regularized technique based on the fracture energy is adopted to overcome the numerical

problems due to the strain and damage localization. A plasticity model with nonlinear isotropic and kinematic hardening, able to reproduce the Baushinger effect, is adopted for the steel of the bars. Furthermore, a plastic bond stress–slip law is introduced for the steel–concrete interfaces. Some numerical examples are developed in order to analyze the axial and bending behavior of reinforced concrete elements under monotonic and cyclic loading and a comparison with experimental results is performed in order to validate the presented material model and numerical procedure.

The paper is organized as follows; initially the elastoplastic-damage model for concrete, the plasticity model for the steel of the bars and the bond stress–slip law for the steel–concrete interface are described. Then, the beam element equations are deduced. The numerical procedure is briefly presented and finally, some numerical applications on reinforced concrete beam elements, subjected to monotonic and cyclic loads, are reported.

2. Reinforced concrete beam

The problem of reinforced concrete beam subjected to axial force and bending moment is considered. In particular, since the axial force and the bending moment are assumed to be constant along the beam span, regularly spaced cracks, at a distance 2λ, can develop because of the limited tensile strength of the concrete; thus, a reference repetitive element, characterized by a length equal to 2λ, can be determined, as shown in Fig. 1. Initially, the crack distance 2λ can be approximately evaluated according to the CEB-FIP Model Code (1990) as function of geometrical and mechanical properties of the beam cross-section. The model and the procedure developed in the next section are able to give a rational evaluation of the crack length 2λ.

The proposed model can be easily extended to the study of reinforced concrete beams also when the axial force and the bending moment are not constant along the span.

Because of the presence of cracks in the beam, elongation e and curvature χ gradients occur inside the repetitive element. Indeed, the study of the beam response can be approached averaging these characteristics along the element.

The structural behavior is determined considering suitable stress–strain relationships for the concrete and for the steel along the beam axis. In particular, the concrete behavior is deduced considering an energy regularization technique, while the response of the steel bar embedded in a concrete cover is determined considering the local effects occurring in the cracked element.

The effect of stirrups is taken into account setting in a suitable way the material parameters governing the constitutive relationship of the concrete. In fact, the presence of transversal reinforcements affects the ductility, i.e. the plastic behavior, and also the compressive strength of the concrete.

Due to the symmetry of the problem, only one half of the repetitive element, characterized by a length λ, is considered in the following; a Cartesian coordinate system (O, x, y, z) with origin in the symmetry section and z defining the beam axis is introduced, as illustrated in Fig. 2. In the following the apex f' indicates the derivative with respect to the z-coordinate, i.e. $f' = \mathrm{d}f/\mathrm{d}z$, while the superimposed dot $\dot{f}$ the derivative with respect to the evolution parameter e.g. the time, $\dot{f} = \mathrm{d}f/\mathrm{d}t$.

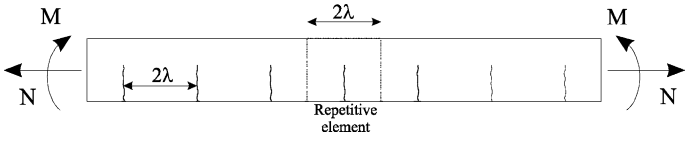

Fig. 1. Reinforced concrete beam subjected to axial force and bending moment: regularly spaced cracks and repetitive element.

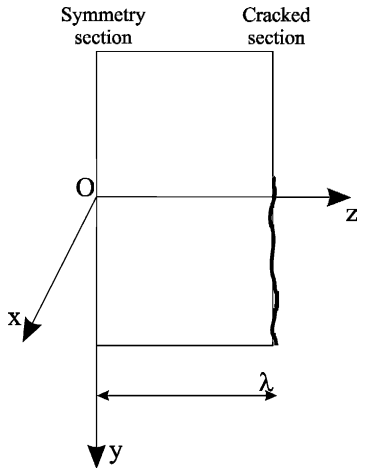

Fig. 2. A half of the repetitive element.

2.1. Concrete model

The concrete presents a strongly nonlinear response. In fact, the tensile behavior is characterized by the development and opening of microcracks, whose coalescence leads to the formation of macrocracks and, hence, of fractures. Moreover, the concrete presents a damage plastic response in compression, due to the development of microcrushes and to the dislocation of the aggregates constituting the concrete. The first phenomenon is responsible for the damage while the second is related to inelastic deformations, which can be reproduced by a plasticity model. A very special feature of the concrete material is the closure of the developed microcracks passing from tensile to compressive loading; this special behavior, often reported as the unilateral effect in the damaged concrete, can be modeled introducing two different damage parameters: one in tension and one in compression. Since the present work deals with the axial and bending behavior of reinforced concrete beams, a one-dimensional constitutive relation is addressed. The free energy is assumed to be:

$$\psi = \eta\left[\frac{1}{2}(1-D_c^+)E_c(\varepsilon_c-\varepsilon_c^p)^2+g^+(\xi^+)\right]+(1-\eta)\left[\frac{1}{2}(1-D_c^-)E_c(\varepsilon_c-\varepsilon_c^p)^2+g^-(\xi^-)+k(\beta_c)\right] \tag{1}$$

where

- ε_c is the total strain in concrete;
- ε_c^p is the concrete plastic strain, so that $\varepsilon_c-\varepsilon_c^p=\varepsilon_c^e$ represents the elastic strain;
- η is the stepwise function of the elastic strain ε_c^e, such that $\eta=1$ if $\varepsilon_c^e\geqslant 0$ and $\eta=0$ if $\varepsilon_c^e<0$;
- the superscript $^+$ corresponds to the case $\eta=1$, i.e. $\varepsilon_c^e\geqslant 0$, and the superscript $^-$ corresponds to the case $\eta=0$, i.e. $\varepsilon_c^e<0$;
- E_c is the Young modulus of the concrete material;
- D_c^+ and D_c^- are the concrete damage parameters in tension and in compression, respectively, satisfying the classical inequalities $0\leqslant D_c^\pm\leqslant 1$, with $D_c^\pm=0$ for the virgin material and $D_c^\pm=1$ for the completely damaged material; moreover, it is assumed $D_c^+\geqslant D_c^-$, i.e. the damage in tension does not induce damage in compression, while the damage in compression leads to a material degradation even in tension, as suggested in Ramtani et al. (1992) and Lee and Fenves (1998) where experimental results are reported;

- ξ^+ and ξ^- are the dimensionless internal parameters governing the concrete damage softening in tension and in compression, respectively;
- β_c is the dimensionless internal parameter governing the strain hardening occurring in compression.

The functions $g^{\pm}(\xi^{\pm})$ and $k(\beta_c)$ are defined as:

$$g^{\pm}(\xi^{\pm}) = \frac{1}{2}E_c \frac{(\varepsilon_0^{\pm})^2}{(1+\alpha^{\pm}\xi^{\pm}-\xi^{\pm})(\alpha^{\pm}-1)} \tag{2}$$

$$k(\beta_c) = \frac{1}{2}K_c\beta_c^2 \tag{3}$$

where $\varepsilon_0^{\pm}$ represents the starting damage threshold strain and $\alpha^{\pm} = \varepsilon_0^{\pm}/\varepsilon_u^{\pm}$ is the threshold ratio, with $\varepsilon_u^{\pm}$ the final damage threshold strain. The quantity K_c is the plastic hardening parameter. The threshold strains $\varepsilon_0^{\pm}$ and $\varepsilon_u^{\pm}$ and the plastic hardening quantity K_c are material parameters. The state laws result:

$$\sigma_c = \frac{\partial\psi}{\partial\varepsilon_c} = \eta[(1-D_c^+)E_c(\varepsilon_c-\varepsilon_c^p)] + (1-\eta)[(1-D_c^-)E_c(\varepsilon_c-\varepsilon_c^p)] \tag{4}$$

$$Y^{\pm} = -\frac{\partial\psi}{\partial D_c^{\pm}} = \frac{1}{2}E_c(\varepsilon_c-\varepsilon_c^p)^2$$

$$\varsigma^{\pm} = -\frac{\partial\psi}{\partial\xi^{\pm}} = \frac{1}{2}E_c\frac{(\varepsilon_0^{\pm})^2}{(1+\alpha^{\pm}\xi^{\pm}-\xi^{\pm})^2}$$

$$t = -\frac{\partial\psi}{\partial\varepsilon_c^p} = \sigma_c$$

$$\vartheta = -\frac{\partial\psi}{\partial\beta_c} = -(1-\eta)K_c\beta_c$$

where σ_c is the stress, $Y^{\pm}$ is the damage energy release rate, $\varsigma^{\pm}$ is the thermodynamical force associated to $\xi^{\pm}$, t is the thermodynamical forces associated to the plastic strain and ϑ is the hardening plastic force. The evolution equations of the internal state variables $(D_c^{\pm}, \xi, \varepsilon_c^p, \beta_c)$ are deduced introducing two damage yield functions F^+ and F^-, one in tension and one in compression, and a plastic yield function F_c^p. In particular, regarding the damage evolutions, it results:

$$F^{\pm}(Y^{\pm},\varsigma^{\pm}) = Y^{\pm}-\varsigma^{\pm} \leqslant 0 \quad \dot{\gamma}^{\pm} \geqslant 0 \quad F^{\pm}\dot{\gamma}^{\pm} = 0 \tag{5}$$

$$\dot{D}_c^{\pm} = \frac{\partial F^{\pm}}{\partial Y^{\pm}}\dot{\gamma}^{\pm} = \dot{\gamma}^{\pm}$$

$$\dot{\xi}^{\pm} = -\frac{\partial F^{\pm}}{\partial\varsigma^{\pm}}\dot{\gamma}^{\pm} = \dot{\gamma}^{\pm}$$

so that $\dot{D}_c^{\pm} = \dot{\xi}^{\pm} = \dot{\gamma}^{\pm}$, i.e. the parameter $\xi^{\pm}$ coincides with the damage internal state variable $D_c^{\pm}$. Taking into account the state law equations (4), the limit condition (5) can be rewritten as:

$$0 = Y^{\pm}-\varsigma^{\pm} = \frac{1}{2}E_c(\varepsilon_c^e)^2 - \frac{1}{2}E_c\frac{(\varepsilon_0^{\pm})^2}{(1+\alpha^{\pm}D_c^{\pm}-D_c^{\pm})^2} \tag{6}$$

which leads to:

$$\varepsilon_{\mathrm{c}}^{\mathrm{e}} = \frac{\varepsilon_0^{\pm}}{1 + \alpha^{\pm} D_{\mathrm{c}}^{\pm} - D_{\mathrm{c}}^{\pm}} \tag{7}$$

i.e.,

$$D_{\mathrm{c}}^{\pm} = \frac{\varepsilon_0^{\pm} - \varepsilon_{\mathrm{c}}^{\mathrm{e}}}{(\alpha^{\pm} - 1)\varepsilon_{\mathrm{c}}^{\mathrm{e}}} = \varepsilon_{\mathrm{u}} \frac{\varepsilon_0^{\pm} - \varepsilon_{\mathrm{c}}^{\mathrm{e}}}{(\varepsilon_0^{\pm} - \varepsilon_{\mathrm{u}}^{\pm})\varepsilon_{\mathrm{c}}^{\mathrm{e}}} \tag{8}$$

Thus, it results $D_{\mathrm{c}}^{\pm} = 0$ for $\varepsilon_{\mathrm{c}}^{\mathrm{e}} = \varepsilon_0^{\pm}$ and $D_{\mathrm{c}}^{\pm} = 1$ for $\varepsilon_{\mathrm{c}}^{\mathrm{e}} = \varepsilon_{\mathrm{u}}^{\pm}$; moreover, substituting the deduced relation (8) into the expression of the stress given by the first equation of the state laws (4), a stress–strain linear softening is obtained when no plastic evolution is considered.

The evolution of the damage parameter $\dot{D}_{\mathrm{c}}^{\pm} = \dot{\xi}^{\pm} = \dot{\gamma}^{\pm}$ is deduced by the consistency equations. In fact, it is:

$$\begin{aligned} &0 = \dot{F}^{\pm}(Y^{\pm}, \varsigma^{\pm}) = \frac{\partial F^{\pm}}{\partial Y^{\pm}} \dot{Y}^{\pm} + \frac{F^{\pm}}{\partial \varsigma} \dot{\varsigma}^{\pm} = \dot{Y}^{\pm} - \dot{\varsigma}^{\pm} = E_{\mathrm{c}} \varepsilon_{\mathrm{c}}^{\mathrm{e}} \dot{\varepsilon}_{\mathrm{c}}^{\mathrm{e}} + E_{\mathrm{c}} \frac{(\varepsilon_0^{\pm})^2 (\alpha^{\pm} - 1)}{(1 + \alpha^{\pm} \xi^{\pm} - \xi^{\pm})^3} \dot{\xi}^{\pm} \\ &\text{with} \quad F^{\pm} = 0 \ \text{ and } \ \dot{\varsigma}^{\pm} > 0 \end{aligned} \tag{9}$$

Taking into account the definitions of the thermodynamical force $\varsigma^{\pm}$ and of the damage energy release rate $Y^{\pm}$, and recalling that $\xi^{\pm} = D_{\mathrm{c}}^{\pm}$, it results:

$$0 = \dot{\varepsilon}_{\mathrm{c}}^{\mathrm{e}} + \frac{(\alpha^{\pm} - 1)\varepsilon_{\mathrm{c}}^{\mathrm{e}}}{(1 + \alpha^{\pm} D_{\mathrm{c}}^{\pm} - D_{\mathrm{c}}^{\pm})} \dot{D}_{\mathrm{c}}^{\pm} \quad \text{with} \quad F^{\pm} = 0 \ \text{ and } \ \dot{D}_{\mathrm{c}}^{\pm} > 0 \tag{10}$$

Substituting expression (8) into Eq. (10), it applies:

$$\dot{D}_{\mathrm{c}}^{\pm} = \frac{\varepsilon_0^{\pm}}{(1 - \alpha^{\pm})(\varepsilon_{\mathrm{c}}^{\mathrm{e}})^2} \dot{\varepsilon}_{\mathrm{c}}^{\mathrm{e}} \quad \text{with} \quad F^{\pm} = 0 \ \text{ and } \ \dot{D}_{\mathrm{c}}^{\pm} > 0 \tag{11}$$

which gives the damage rate as function of the elastic strain rate. For what concerns the plasticity evolution, it is assumed:

$$F_{\mathrm{c}}^{\mathrm{p}}(\sigma_{\mathrm{c}}, \vartheta) = -\frac{\sigma_{\mathrm{c}}}{(1 - D_{\mathrm{c}}^{-})} + \vartheta - f_{\mathrm{c}} \leqslant 0 \quad \text{with} \quad \dot{\mu}_{\mathrm{c}} \geqslant 0 \ \text{ and } \ F_{\mathrm{c}}^{\mathrm{p}} \dot{\mu}_{\mathrm{c}} = 0 \tag{12}$$

$$\begin{aligned} \dot{\varepsilon}_{\mathrm{c}}^{\mathrm{p}} &= \frac{\partial F_{\mathrm{c}}^{\mathrm{p}}}{\partial \sigma_{\mathrm{c}}} \dot{\mu}_{\mathrm{c}} = -\frac{\dot{\mu}_{\mathrm{c}}}{1 - D_{\mathrm{c}}^{-}} \\ \dot{\beta}_{\mathrm{c}} &= \frac{F_{\mathrm{c}}^{\mathrm{p}}}{\partial \vartheta} \dot{\mu}_{\mathrm{c}} = \dot{\mu}_{\mathrm{c}} \end{aligned} \tag{13}$$

such that, it results:

$$\dot{\beta}_{\mathrm{c}} = -(1 - D_{\mathrm{c}}^{-}) \dot{\varepsilon}_{\mathrm{c}}^{\mathrm{p}} \tag{14}$$

The quantity $\sigma_{\mathrm{c}}/(1 - D_{\mathrm{c}}^{-}) = \tilde{\sigma}_{\mathrm{c}}$ in Eq. (12) is the effective stress in compression, while f_{c} is the effective plastic yield stress of the concrete. The consistency condition for the plastic process leads to:

$$\begin{aligned} 0 &= \dot{F}_{\mathrm{c}}^{\mathrm{p}}(\sigma_{\mathrm{c}}, \vartheta) = \frac{\partial F_{\mathrm{c}}^{\mathrm{p}}}{\partial \sigma_{\mathrm{c}}} \dot{\sigma}_{\mathrm{c}} + \frac{\partial F_{\mathrm{c}}^{\mathrm{p}}}{\partial \vartheta} \dot{\vartheta} = \frac{1}{1 - D_{\mathrm{c}}^{-}} \dot{\sigma}_{\mathrm{c}} + \dot{\vartheta} = \frac{1}{1 - D_{\mathrm{c}}^{-}} \left[(1 - D_{\mathrm{c}}^{-}) E_{\mathrm{c}} (\dot{\varepsilon}_{\mathrm{c}} - \dot{\varepsilon}_{\mathrm{c}}^{\mathrm{p}}) \right] - K_{\mathrm{c}} \dot{\beta}_{\mathrm{c}} \\ &= E_{\mathrm{c}} (\dot{\varepsilon}_{\mathrm{c}} - \dot{\varepsilon}_{\mathrm{c}}^{\mathrm{p}}) + K_{\mathrm{c}} (1 - D_{\mathrm{c}}^{-}) \dot{\varepsilon}_{\mathrm{c}}^{\mathrm{p}} \end{aligned} \tag{15}$$

Solving Eq. (15) with respect to $\dot{\varepsilon}_c^p$, the evolution equations of the plastic process result:

$$\begin{aligned}\dot{\varepsilon}_c^p &= H_c^- \dot{\varepsilon}_c \\ \dot{\beta}_c &= -(1 - D_c^-) H_c^- \dot{\varepsilon}_c\end{aligned} \tag{16}$$

where

$$H_c^- = \frac{E_c}{E_c + K_c(1 - D_c^-)} \tag{17}$$

Finally, the damage rate in tension and in compression can be computed in terms of the total strain rate as:

$$\dot{D}_c^{\pm} = \frac{\varepsilon_0^{\pm}}{(1 - \alpha^{\pm})(\varepsilon_c^e)^2}(\dot{\varepsilon}_c - \dot{\varepsilon}_c^p) = \frac{\varepsilon_0^{\pm}}{(1 - \alpha^{\pm})(\varepsilon_c^e)^2}(1 - H_c^{\pm})\dot{\varepsilon}_c \tag{18}$$

where $H_c^+ = 0$. Note that the specialization of formula (18) in the tensile case leads to Eq. (11), as $\dot{\varepsilon}_c^e = \dot{\varepsilon}_c$ in tension. The tangent constitutive modulus E_c^t is obtained by differentiating the stress–strain relationship $(4)_1$:

$$E_c^t = \left[(1 - D_c^{\pm}) - \frac{\varepsilon_0^{\pm}}{(1 - \alpha^{\pm})\varepsilon_c^e}\right] \frac{E_c K_c (1 - D_c^-)}{E_c + K_c(1 - D_c^-)}$$

In Fig. 3 it is schematically reported the stress–strain response of the concrete model in compression and in tension, emphasizing the behavior under loading–unloading cycles. Finally, all state and evolution equations of the concrete model are summarized in Table 1.

It can be noted that the strain and stress along any concrete string are assumed to be constant, i.e. they do not depend on the z-coordinate. Indeed, denoting by $w_c(x, y, z)$ the horizontal displacement of a typical point lying on the cross-section sited at a distance z form the symmetry section, it results:

$$w_c(x, y, z) = z\varepsilon_c(x, y) \tag{19}$$

At the cracked section it applies:

$$w_c(x, y, \lambda) = \lambda\varepsilon_c(x, y) = \lambda(\varepsilon_c^d(x, y) + \varepsilon_c^{ep}(x, y)) \tag{20}$$

where the elasto-plastic strain ε_c^{ep}, comprising both elastic and plastic strain, is introduced. The elasto-plastic horizontal displacement w^{ep} at the typical cross-section is obtained as $w^{ep}(x, y) = z\varepsilon_c^{ep}(x, y)$. The

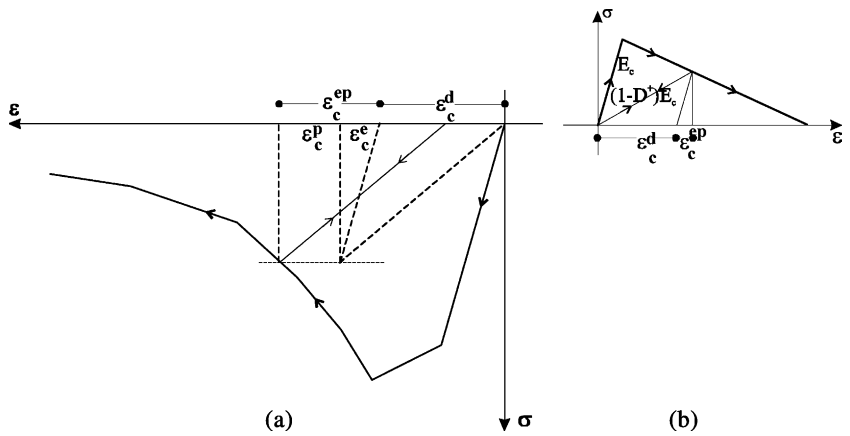

Fig. 3. Stress–strain response of the concrete model in compression (a) and in tension (b), under loading–unloading cycles.

Table 1
State and evolution equations of the concrete model

$$\sigma_c = \eta[(1 - D_c^+)E_c(\varepsilon_c - \varepsilon_c^p)] + (1 - \eta)[(1 - D_c^-)E_c(\varepsilon_c - \varepsilon_c^p)]$$

$$F^\pm = Y^\pm - \varsigma^\pm = \frac{1}{2}E_c(\varepsilon_c^e)^2 - \frac{1}{2}E_c\frac{(\varepsilon_0^\pm)^2}{(1 + \alpha^\pm D_c^\pm - D_c^\pm)^2} \leqslant 0$$

$$\dot{D}_c^\pm = \frac{\varepsilon_0^\pm}{(1 + \alpha^\pm)(\varepsilon_c^e)^2}(\dot{\varepsilon}_c - \dot{\varepsilon}_c^p) \quad \text{with } F^\pm = 0$$

$$F_c^p = -\frac{\sigma_c}{(1 - D_c^-)} - K_c\beta_c - f_c \leqslant 0$$

$$\dot{\varepsilon}_c^p = \frac{E_c}{E_c + K_c(1 - D_c^-)}\dot{\varepsilon}_c \quad \text{with } F_c^p = 0$$

$$\dot{\beta}_c = -(1 - D_c^-)\frac{E_c}{E_c + K_c(1 - D_c^-)}\dot{\varepsilon}_c$$

strain $\varepsilon_c^d = \varepsilon_c - \varepsilon_c^{ep}$ reflects the strain corresponding to stiffness degradation in consequence of damage, as schematically shown in Fig. 3. The elasto-plastic strain is obtained as:

$$\varepsilon_c^{ep} = (1 - D_c^\pm)\varepsilon_c + D_c^\pm\varepsilon_c^p \tag{21}$$

Indeed, the concrete damage is localized in a zone close to the fracture or crashing section, i.e. at $z = \lambda$. The size ℓ of the damaged zone is a material parameter. Let $G_F^\pm$ be the specific fracture energy dissipated in the damaged zone of length ℓ in tension and in compression. The slopes of the softening branches in tension and in compression of the proposed constitutive model for the concrete, and in particular the parameters $\varepsilon_u^\pm$ are properly set in order to have the same damage dissipation $G_F^\pm$ for the whole string of length 2λ:

$$0.5E_c\varepsilon_0^\pm\varepsilon_u^\pm = \frac{G_F^\pm}{2\lambda} \tag{22}$$

in such a way, the constitutive law is able to reproduce the overall behavior of a string characterized by a length 2λ.

On the other hand, the size ℓ of the zone associated with damage effects can be considered small with respect to λ, i.e. $\ell \ll \lambda$, thus it can be assumed $\ell = 0$. In other words, it is assumed that the fracture or the crash localize in a section.

2.2. Steel model

A plasticity model for the steel, based on the formulation developed by Yoshida et al. (2002), is proposed. It considers nonlinear isotropic and kinematic hardening, and it is able to reproduce the Baushinger effect.

The stress–strain relationship is:

$$\sigma_s = E_s(\varepsilon_s - \varepsilon_s^p) \tag{23}$$

where ε_s and ε_s^p are the total and the plastic axial strain of the steel bar, respectively, and E_s is the steel Young modulus. Denoting by w the displacement field of the bar, the axial strain is $\varepsilon_s = w'$. The plasticity yield function, characterized by an isotropic and kinematic hardening, is:

$$F_s^p(\sigma_s, q_s, \delta_s) = |\sigma_s - q_s| - (\delta_s + f_s) \leqslant 0 \tag{24}$$

where f_s is the steel yield stress, q_s is the so-called back stress, and δ_s is the isotropic hardening force.

The plastic strain evolution is governed by the following equations:

$$F_s^p(\sigma_s, q_s, \delta_s) \leqslant 0 \quad \dot{\mu}_s \leqslant 0 \quad F_s^p \dot{\mu}_s = 0 \tag{25}$$

$$\begin{aligned} \dot{\varepsilon}_s^p &= \frac{\partial F_s^p}{\partial \sigma_s} \dot{\mu}_s = \dot{\mu}_s \mathrm{sign}(\sigma_s - q_s) \\ \dot{\delta}_s &= [m_s(\delta_{sat} - \delta_s) + K_s]\dot{\mu}_s \\ \dot{q}_s &= C_s \left[\frac{a_s}{\delta_s + \sigma_s} |\sigma_s - q_s| - q_s \right] \dot{\varepsilon}_s^p \end{aligned} \tag{26}$$

with $\dot{\mu}_s$, the plastic multiplier; β_s, the effective plastic strain; K_s, m_s and δ_{sat}, the isotropic hardening constants; C_s and a_s, the kinematic hardening parameters. From the consistency condition the plastic multiplier $\dot{\mu}_s$ is determined.

The parameters C_s and a_s are assumed to be function of the effective plastic strain β_s as:

$$\begin{aligned} C_s &= C_{final} + \left(1 + \frac{C_{start} - C_{final}}{C_{final}} e^{(-\beta_s C_{exp})} \right) \\ a_s &= a_{final} + \left(1 + \frac{a_{start} - a_{final}}{a_{final}} e^{(-\beta_s a_{exp})} \right) \end{aligned} \tag{27}$$

where C_{start}, C_{final}, a_{start} and a_{final} are the initial and final value of C_s and a_s, respectively and C_{exp} and a_{exp} are material constants. The values of the parameters C_s and a_s are updated using formula (27) during the unloading phases, i.e. when $\sigma_s \cdot \dot{\sigma}_s < 0$.

It is worth noting that also the proposed steel model can be set in the framework of thermodynamics (Lemaitre and Chaboche, 1990), but this formulation is herein omitted, for brevity.

2.3. Steel–concrete interface

A very important role in the overall response of the reinforced beam is played by the bond-slip between the concrete and the steel bar. For the typical steel bar positioned at a point of the cross-section with the coordinates x, y, the slip is defined as:

$$s(x, y, z) = w(x, y, z) - w^{ep}(x, y, z) = w(x, y, z) - z\varepsilon_c^{ep}(x, y) \tag{28}$$

It can be emphasized that the mechanical phenomena occurring at the steel–concrete interface are complex. For low values of the stresses at the interface, the bond efficiency is ensured mostly by chemical adhesion; this phase can be modeled by a linear elastic behavior. For higher values of the stresses the chemical adhesion breaks down and microcraks originate. A rather sudden reduction of the bond stress, depending on the confinement effect, occurs; a damage model could be adopted to simulate this mechanical behavior (Soh et al., 1999). Increasing the slip values, the bond behavior tends to become dry-friction type, since the concrete between the steel lugs is crushed; the dry-friction effect can be modeled by plasticity.

Indeed, the modeling of the steel–concrete interface behavior would require the use of both damage and plasticity theories. In order to define a simple but effective model, only the plasticity effect is considered, as it mainly affects the ultimate behavior of the bond-slip. In particular, the model proposed by Ciampi et al. (1981), adopted by the CEB-FIP Model Code (1990) and by the EUROCODE 2 (1993), is herein framed in the plasticity theory.

The interface constitutive tangential stress–slip relationship is written as:

$$\tau = K_\tau (s - s_p) \tag{29}$$

where s_p represents the interface plastic slip, whose evolution is governed by the following equations:

$$\dot{\mu}_\tau \geqslant 0 \quad F_\tau \leqslant 0 \quad F_\tau \dot{\mu}_\tau = 0 \tag{30}$$

with F_τ, the yield function and $\dot{\mu}_\tau$, the plastic multiplier. The slip yield function is set as follows:

- when $\tau, s \geqslant 0$, it is assumed:

$$F_\tau = |\tau| - \left[\tau_1(\beta) + \frac{\tau_1(\beta)-\tau_3}{s_1}(\alpha - s_1)^- - \frac{\tau_1(\beta)-\tau_3}{s_3 - s_2}\frac{(\alpha - s_3)^-}{\alpha - s_3}(\alpha - s_2)^+ - (\tau_1(\beta)-\tau_3)\frac{(\alpha - s_3)^+}{\alpha - s_3}\right] \tag{31}$$

with $(\bullet)^+$ and $(\bullet)^-$ the positive and negative part of a number and

$$\begin{aligned}
&\tau_1(\beta) = \tau_3 - \frac{\tau_1 - \tau_3}{s_3}(\beta - s_3)^- \\
&\dot{\mu}_\tau = \frac{K_\tau \operatorname{sign}(\tau)}{K_\tau + \Pi}\dot{s} \\
&\dot{\alpha} = \dot{\mu}_\tau \\
&\dot{s}_p = \dot{\mu}_\tau \operatorname{sign}(\tau) = \frac{K_\tau}{K_\tau + \Pi}\dot{s} \\
&\Pi = \frac{\tau_1(\beta)-\tau_3}{s_1}\frac{(\alpha - s_1)^-}{\alpha - s_1} - \frac{\tau_1(\beta)-\tau_3}{s_3 - s_2}\frac{(\alpha - s_3)^-}{\alpha - s_3}\frac{(\alpha - s_2)^+}{\alpha - s_2}
\end{aligned} \tag{32}$$

- when $\tau, s < 0$, it is assumed:

$$F_\tau = |\tau| - \tau_3 \tag{33}$$

with

$$\begin{aligned}
&\dot{\mu}_\tau = \operatorname{sign}(\tau)\dot{s} \\
&\dot{\beta} = \dot{\mu}_\tau \\
&\dot{s}_p = \dot{\mu}_\tau \operatorname{sign}(\tau) = \dot{s}
\end{aligned} \tag{34}$$

In Eqs. (31)–(34) the quantities τ_1, τ_3, s_1, s_2, s_3 and K_τ are interface parameters. The piecewise linear response of the interface model and the mechanical interpretation of the material parameters τ_1, τ_3, s_1, s_2 and s_3 are schematically reported in Fig. 4. Two possible loading histories are reported: path 1 represents a monotonic slip history, while path 2 corresponds to a cyclic slip history.

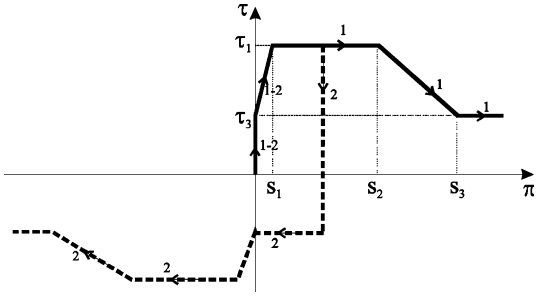

Fig. 4. Schematic mechanical response of the concrete–steel interface: plastic slip versus tangential stress.

3. RC beam equations

The concrete, the steel and the interface constitutive laws, developed in the previous section, are adopted to study the softening behavior of reinforced concrete beams. In particular, beam cross-sections, involving two steel reinforcements and presenting a symmetry axis y, are considered. Let y_1 and y_2 denote the coordinates in the cross-section where the reinforcements are positioned. Note that the study can be extended to other geometries of the cross-section and, moreover, the presence of any other steel bar can be considered. The kinematics of the beam is completely described by the elongation e and the bending curvature χ, such that the strain at a typical point of the beam is:

$$\varepsilon = e + y\chi \tag{35}$$

By compatibility, it occurs $\varepsilon = \varepsilon_c$.

The axial force N_c and the bending moment M_c in the concrete at the cracked cross-section, are evaluated as:

$$\begin{aligned} N_c(e,\chi) &= \int_{A_c} \sigma_c(e,\chi)\,\mathrm{d}A \\ M_c(e,\chi) &= \int_{A_c} y\sigma_c(e,\chi)\,\mathrm{d}A \end{aligned} \tag{36}$$

where A_c is the cross-section area of the concrete beam.

The axial force N_s and the bending moment M_s in the steel reinforcements at the cracked cross-section are:

$$\begin{aligned} N_s &= F_1 + F_2 \\ M_s &= y_1F_1 + y_2F_2 \end{aligned} \tag{37}$$

where F_i is the force due to the ith steel bar acting on the cross-section at $z = \lambda$.

The differential equilibrium equation of the ith steel bar, characterized by area A_i and circumference S_i, with $i = 1, 2$, is:

$$A_i\sigma_s' + S_i\tau = 0 \tag{38}$$

subjected to the boundary conditions:

$$\begin{aligned} &w_i = 0 \quad \text{at } z = 0 \\ &A_i\sigma_s = F_i \quad \text{at } z = \lambda \end{aligned} \tag{39}$$

The differential equation (38), subjected to boundary condition (39), is discretized in finite elements.

Finally, the behavior of the cross-section softening beam is governed by the equilibrium equations:

$$\begin{aligned} N_c + N_s - \phi N_{ext} &= \int_{A_c} \sigma_c(e,\chi)\,\mathrm{d}A + F_1 + F_2 - \phi N_{ext} = 0 \\ M_c + M_s - \phi M_{ext} &= \int_{A_c} y\sigma_c(e,\chi)\,\mathrm{d}A + y_1F_1 + y_2F_2 - \phi M_{ext} = 0 \end{aligned} \tag{40}$$

where N_{ext} and M_{ext} are the external axial force and bending moment, respectively, and ϕ is the loading multiplier, introduced with the aim of developing an arc-length procedure.

It can be emphasized that the beam elongation e and curvature χ and the displacements of the two bars are related by suitable kinematic compatibility equations, derived from the classical plane section hypothesis of the Euler–Bernoulli beam theory.

Furthermore, in order to verify the accuracy of the assumed value for the cracking distance 2λ, the stress in the concrete at the section $z = 0$ is computed. The forces F_1^0 and F_2^0 acting in the steel bars at the uncracked section are evaluating using the equilibrium equations as:

$$F_i^0 = F_i - \int_0^\lambda S_i \tau \, \mathrm{d}z \tag{41}$$

with $i = 1,2$. The axial force N_s^0 and the bending moment M_s^0 in the steel at $z = 0$ are:

$$N_s^0 = F_1^0 + F_2^0 \quad M_s^0 = y_1 F_1^0 + y_2 F_2^0 \tag{42}$$

As a consequence the axial force N_c^0 and the bending moment M_c^0 in the concrete at $z = 0$ are:

$$N_c^0 = \phi N_{\text{ext}} - N_s^0 \quad M_c^0 = \phi M_{\text{ext}} - M_s^0 \tag{43}$$

Once N_c^0 and M_c^0 are computed, the stress in the concrete is determined applying the classical Navier formula, assuming a linear elastic response for the concrete. If the maximum tensile stress is greater than the tensile strength of the concrete, the section at $z = 0$ is also damaged and the crack distance 2λ must be reduced.

The reinforced concrete beam response is governed by the nonlinear system of equations obtained considering the equilibrium conditions of the bars and of the cross-section and the kinematic compatibility equations. The nonlinear problem is solved developing a numerical procedure. The unknowns of the problem, i.e. the nodal displacements of the bars, the global kinematic parameters e, χ defining the average beam deformation and steel forces F_1, F_2 due to the bar actions in the cross-section at $z = \lambda$, are determined adopting a Newton–Raphson algorithm, taking into account the constraint equations provided by the arc-length method.

The softening behavior of the material constituting the beam, in fact, can induce an overall response characterized by steep softening and snap-back branches. Hence, it appears convenient to adopt an arc-length method able to catch the overall beam response. In particular, the cylindrical as well as the linearized arc-length methods (Crisfield, 1991) with local control are developed for the particular problem under consideration. Special attention is addressed to the choice of the control parameters which represents a key point of the arc-length method. The two strains $\hat{\varepsilon}_c^+$ and $\hat{\varepsilon}_c^-$, evaluated at $y = y_u^+$ and $y = y_u^-$, are assumed as control parameters. The coordinates y_u^+ and y_u^- define the position of the axes in the cross-section where the elastic strains computed at the time t_n are equal to the tensile and compressive final damage threshold strains, respectively, i.e. $\varepsilon_{c,n}^e(y_u^+) = \varepsilon_u^+$ and $\varepsilon_{c,n}^e(y_u^-) = \varepsilon_u^-$.

If the coordinates y_u^+ and y_u^- are not internal to the cross-section it is assumed $y_u^+ = \pm h/2$ and $y_u^- = \mp h/2$, where h is the dimension of the cross-section along the y-axis and the sign + or − is selected in dependence on the sign of the external load.

The time integration of evolutive equations of the concrete, of the steel and of the steel–concrete interface in the interval $[t_n, t_{n+1}]$ is performed adopting a backward-Euler scheme (Simo and Hughes, 1998).

In the following some details regarding the time integration of the damage–plastic evolutive equations governing the concrete behavior are reported.

The discretized forms of the evolution equations of the plastic strain $(16)_1$ and of the damage (18) are:

$$\begin{aligned} \varepsilon_c^p &= \varepsilon_{c,n}^p + H_c^\pm \Delta\varepsilon_c \\ D_c^\pm &= D_{c,n}^\pm + \frac{\varepsilon_0^\pm}{(1-\alpha^\pm)(\varepsilon - \varepsilon_c^p)^2}(1 - H_c^\pm)\Delta\varepsilon_c \end{aligned} \tag{44}$$

where $H_c^\pm$ is defined in Section 2.1. The solution of the coupled equations (44) is performed by means of a return-mapping algorithm, i.e. a predictor–corrector procedure (Simo and Hughes, 1998).

Depending on the trial values of limit functions $F_c^{p^{tr}}$ and $F^{\pm tr}$, computed assuming no plastic and damage evolution, four different cases can occur.

Case 1: $F_c^{p^{tr}} < 0$ $F^{\pm tr} < 0$. The damage and yield functions are satisfied so there is neither plastic flow nor damage evolution. The elastic trial state is the solution of the damage plastic problem at this step.

Case 2: $F_c^{p^{tr}} < 0$ $F^{\pm tr} \geqslant 0$. The damage limit function is not satisfied. In this case, only damage evolution arises; in fact, in tension, there is never plastic evolution; moreover in compression, it can be noted that the plastic yield function does not depend on the value of $D_c^{\pm}$; thus, updating the variable $D_c^{\pm}$, the value of the plastic yield function does not change, i.e. $F_c^p = F_c^{p^{tr}} < 0$, and no plastic evolution occurs. Finally, the solution of case 2 is computed solving Eq. $(44)_2$ with $\varepsilon_c^p = \varepsilon_{c,n}^p$, under the constraints $D_c^{\pm} \geqslant D_{c,n}^{\pm}$ and $0 \leqslant D_c^{\pm} \leqslant 1$.

Case 3: $F_c^{p^{tr}} \geqslant 0$ $F^{\pm tr} < 0$. This case can occur only in compression. The plastic evolution is evaluated solving Eq. $(44)_1$ with $D_c^- = D_{c,n}^-$. Once ε_c^p is computed, a new value of the trial damage limit function $F^{\pm tr}$ is determined. If $F^{\pm tr} < 0$, then only plastic evolution occurs.
On the contrary, if $F^{\pm tr} \geqslant 0$, also a damage evolution occurs and the evaluation of the plastic and damage increments is performed solving case 4.

Case 4: $F_c^{p^{tr}} \geqslant 0$ $F^{\pm tr} \geqslant 0$. Also this case can occur only in compression. The plastic strain and damage evolutions are evaluated solving the coupled nonlinear evolutive Eq. (44) under the constraints $\varepsilon_c^p \leqslant \varepsilon_{c,n}^p$, $D_c^- \geqslant D_{c,n}^-$ and $0 \leqslant D_c^- \leqslant 1$. To this end, the Newton-Raphson algorithm is adopted.

The time integration of the nonlinear plastic evolutive equations governing the steel behavior is performed using a Newton–Raphson algorithm, as the equations, reported in formulas (26), result coupled.

4. Numerical studies

Numerical applications are developed to analyze the behavior of typical steel reinforced concrete beams. The axial and bending behavior under monotonic and cyclic loading is investigated. Steel reinforced concrete elements characterized by a rectangular cross-section and by different amounts of steel reinforcements are studied.

4.1. Axial and bending behavior

The following material data are adopted:

- Concrete:

  $E_c = 30{,}000$ MPa $\quad f_c = 15$ MPa $\quad K_c = 10{,}000$ MPa $\quad \varepsilon_0^+ = 0.00007$ $\quad \varepsilon_0^- = -0.00084$

  $\varepsilon_u^+ = 0.00025$ $\quad \varepsilon_u^- = -0.002$

- Steel:

  $E_s = 210{,}000$ MPa $\quad \sigma_s = 440$ MPa $\quad K_s = 1850$ MPa $\quad m_s = \delta_{sat} = 0.0$ $\quad C_{start} = C_{final} = 0.0$

  $a_{start} = a_{final} = 0.0$ MPa

- Steel–concrete interface:

  $K_\tau = 250$ N/mm^3 $\quad \tau_1 = 10$ MPa $\quad \tau_2 = 2.5$ MPa $\quad s_1 = 0.6$ mm $\quad s_2 = 2.0$ mm $\quad s_3 = 3.5$ mm

It is worth noting that in the following applications only isotropic linear hardening is considered for the steel, as pointed out by the previous material data.

The geometrical data are set as:

$$\lambda = 200 \text{ mm} \quad b = 300 \text{ mm} \quad h = 600 \text{ mm} \quad y_1 = -270 \text{ mm} \quad y_2 = 270 \text{ mm}$$

where b and h are the width and the height of the rectangular cross-section, respectively.

The material parameters for concrete are set on the basis of the following considerations:

- the tensile strength $E_c\varepsilon_0^+ = 2.1$ MPa and the fracture energy $G_F^+ = 0.1$ N/mm are adopted in tension;
- the parameters governing the constitutive law in compression are set on the basis of the concrete behavior proposed by Park and Paulay (1975) (see Fig. 5).

Two beam elements characterized by different reinforcements are investigated; the first element C1 is reinforced by 2 bars ∅16 at the bottom and 2 bars ∅16 at the top; the second element, named C2, is reinforced by 4 bars ∅16 at the bottom and 4 bars ∅16 at the top.

4.1.1. Axial behavior

The tensile mechanical behavior of steel reinforced elements is analyzed. First a monotonic load is applied.

In Fig. 6 the axial force versus the average axial strain along the element is plotted for the two different analyzed elements; in particular, the total axial force, the axial force in concrete and in the reinforcements are represented. It can be pointed out that in both the analyses when the damage starts to propagate in concrete, slip occurs at the steel–concrete interfaces and the mechanical response of the element is characterized by a softening branch. When the section is completely damaged the overall mechanical response is governed only by the reinforcement behavior. For the C1 element the softening branch is steeper than for the C2 one, while the concrete response in the two analyses is exactly the same. Further analyses, not reported here, have shown that increasing the amount of steel reinforcement the post-peak branch reduces its slope and it tends to become flat.

In Figs. 7 and 8 the slip and the steel strain along the bars are plotted at several steps of the analysis, respectively, for the C2 reinforced element. As soon as damage starts to propagate in concrete ($e > 0.00007$)

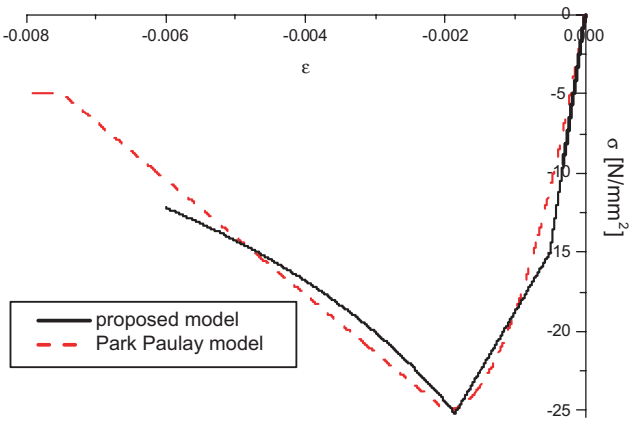

Fig. 5. Comparison between the adopted constitutive model in compression and the one proposed by Park and Paulay (1975).

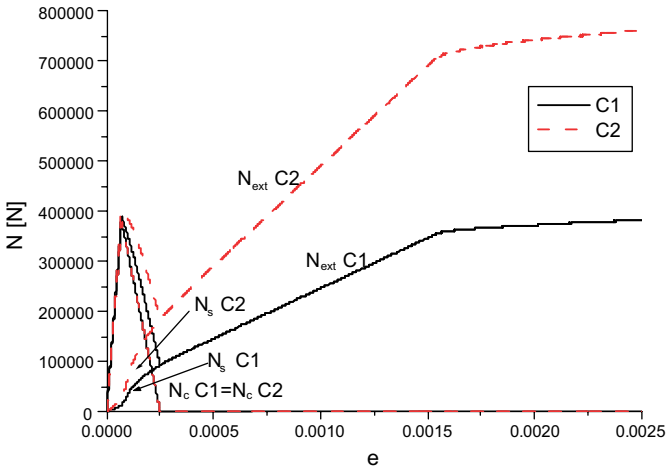

Fig. 6. Axial force versus average axial strain for two different beam elements.

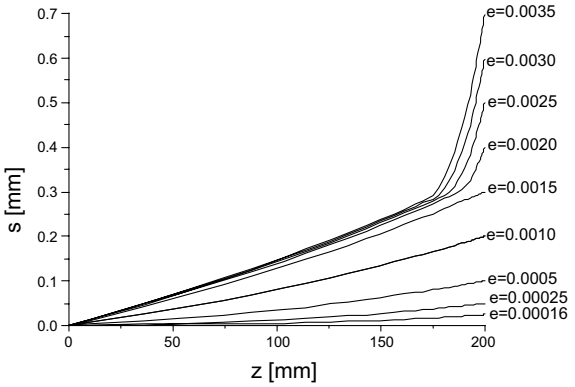

Fig. 7. Slip along the concrete–steel interfaces at different steps of the analysis, for the C2 element.

slip occurs along the bars; then, when the section is completely damaged ($e > 0.00025$) and when plasticity occurs in the bars ($e > 0.0015$), the slip at the interface and the strain in the bars become more significant and they tend to concentrate in a narrow zone close to the cracked section. It can be pointed out that only a narrow zone of the bars is interested by plastic strains, while the greater part of the reinforcements still behaves elastically. This last phenomenon is of topical interest in concrete structures, as it can lead to brittle failure due to the localization of steel strains near cracks. In this case the ultimate strain in the steel can be achieved near the crack, when the related average value is still elastic, avoiding the expected and required spread of plasticity along the rebars.

In Fig. 9 the axial response of the C2 element subjected to a cyclic load is plotted. In particular, tension load, followed by compression load and by tension again are provided. In that figure, the total axial force, the axial force in concrete and in the reinforcements are plotted versus the axial elongation. It can be pointed out that:

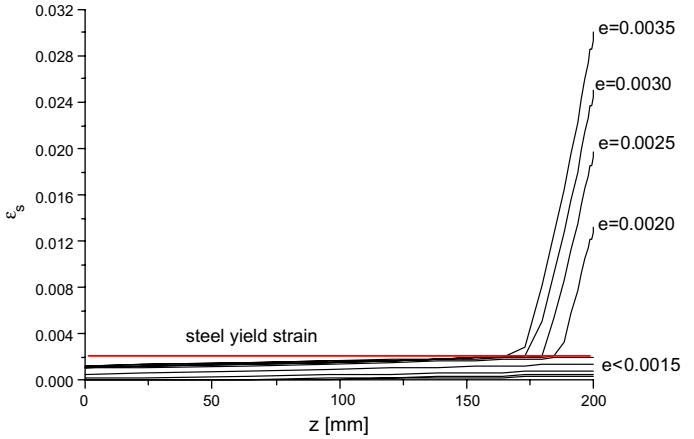

Fig. 8. Strain in the reinforcement bars at different steps of the analysis, for the C2 element.

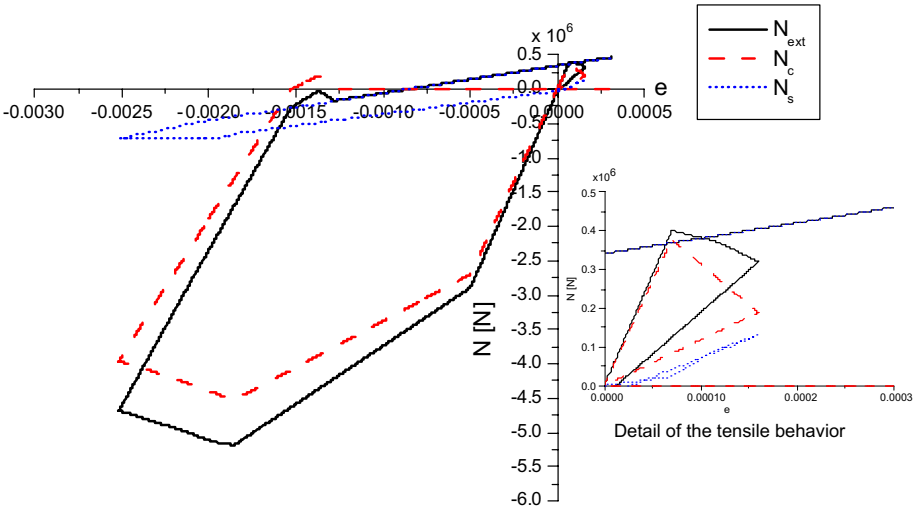

Fig. 9. Axial force versus average axial strain under cyclic loading, for the C2 element.

- at the beginning of the analysis, during the tensile loading, the overall mechanical response is characterized by a softening branch since damage starts to occur in concrete; in this phase the steel reinforcements still behave elastically; it is worth noting that the N_s axial force, represented in Fig. 9, is related to the rebars embedded in concrete, so it takes account of the bond stress distribution developed along the interfaces;
- the residual axial strain for $N_{ext} = 0$ is due to residual slip at the interfaces (see detail in Fig. 9);
- when a compressive load is applied, the initial stiffness of the element is recovered since the crack closure occurs in concrete material;
- during the compressive load the overall mechanical response is influenced first by the plasticity and the damage occurring in concrete and finally by the plasticity in the steel reinforcements;

- during the reloading in tension the element stiffness depends on the accumulated tensile damage, in fact, this branch is parallel to the unloading tensile branch of the first cycle; then, damage keeps on propagating and when the cracked section is completely damaged the overall mechanical response is governed only by the reinforcement behavior.

In all the developed analyses the accuracy of the assumed value for the cracking distance 2λ has been verified computing the stress in the concrete at the section $z = 0$.

4.1.2. Bending behavior

The bending behavior of the C2 reinforced element is investigated under monotonic and cyclic loading.

In Fig. 10 the bending moment versus the average curvature along the element is plotted. The element behavior, obtained by the proposed model that takes into account the steel–concrete interface, is compared with the classical section behavior, obtained considering only the beam cross-section. It can be pointed out that:

- the pre-cracking behavior, obtained with the two approaches, are obviously the same in the two analyses (see the detail in Fig. 10);
- in the post-cracking range the section analysis provides a value of the curvature higher than the one resulting from the element analysis for the same bending moment; this aspect is due to the stiffness effect given by the tensile concrete between two cracks;
- significant differences appear from the yielding stage up to failure both in terms of strength and deformation.

In Fig. 11 the bond stress at the steel–concrete interface versus the curvature is represented for the compressed and tensile reinforcements. Note that for a positive bending moment the reinforcement at the bottom results in tension while the one at the top in compression. It can be pointed out that for very low values of the curvature as soon as damage occurs in the tensile part of the section, slip and tangential stress

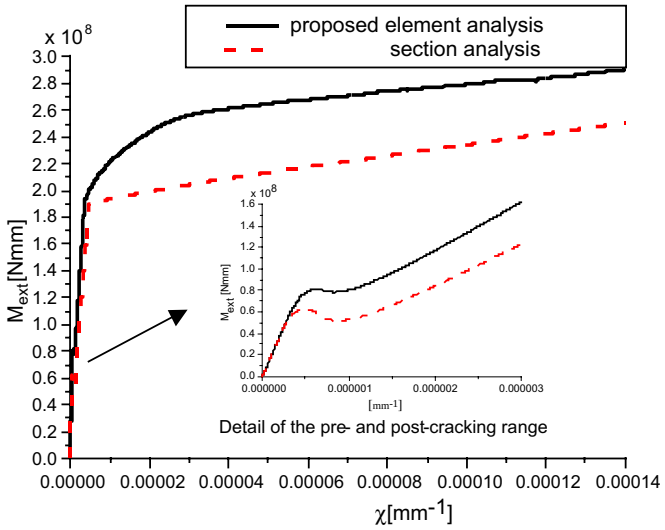

Fig. 10. Bending moment versus average curvature, for the C2 element: comparisons between the proposed element analysis and the section analysis.

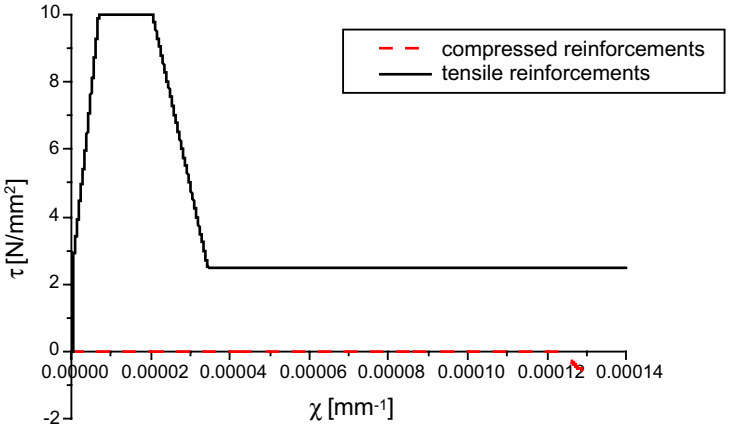

Fig. 11. Bond stress at the concrete–steel interface versus average curvature for the compressed and tensile reinforcements.

appear at the steel–concrete interface at the bottom of the section. For $\chi \geqslant 0.00012$ mm^{-1}, when the compressive part of the section starts to damage, bond stresses appear also at the steel–concrete interface at the compressive edge of the section.

In Figs. 12 and 13 the bending response of the C2 concrete element under cyclic loading is represented. In particular, the total bending moment, the bending moment in concrete and in the reinforcements are reported. In Fig. 12 the unloading branch starts after the tensile concrete cracking and before the steel yielding. At the end of the first loading phase, the tensile part of the section is significantly damaged. Then, when the external moment becomes negative, during the unloading phase, the initial bending stiffness is recovered since the model accounts for the crack closure. At the end of the unloading phase the cracked section is completely damaged in tension. During the reloading phase, for a curvature belonging to the range $-6.8 \times 10^{-7} < \chi < 3.3 \times 10^{-7}$, the whole concrete section is in tension, so only the rebars react to the external moment ($M_c = 0$, $M_{ext} = M_s$).

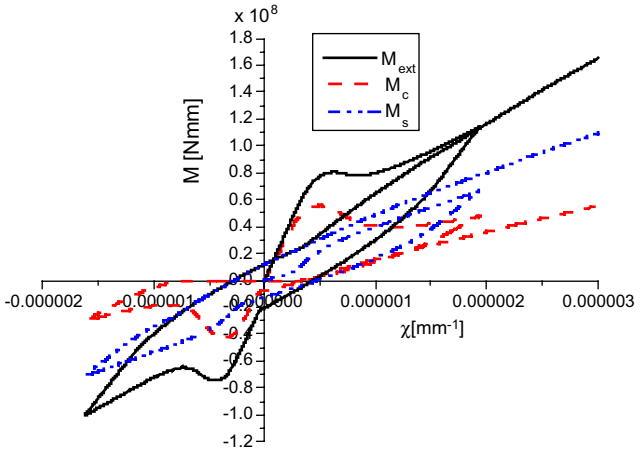

Fig. 12. Bending moment versus curvature for the first cyclic loading, for the C2 element.

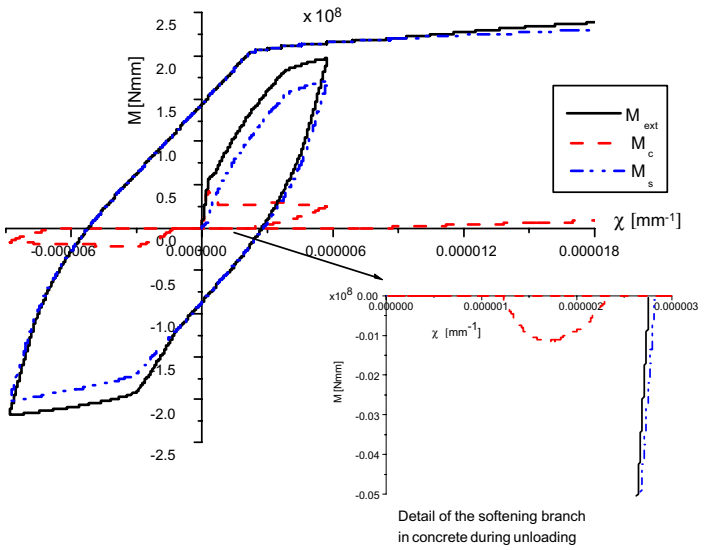

Fig. 13. Bending moment versus average curvature for the second cyclic loading, for the C2 element.

In Fig. 13 the unloading branch starts after the steel yielding in tension. In this case, at the beginning of the unloading path the greater part of the section is already damaged in tension. After the softening branch of the concrete bending moment M_c, during the unloading phase reported in the detail, the section results completely damaged in tension. When the average curvature varies from 1.22×10^{-6} to -1.11×10^{-6}, unloading, and from -6.11×10^{-6} to 8.27×10^{-6}, reloading, the whole section is in tension. This aspect can be highlighted in Fig. 14 where the strains at the top ε_c^T and at the bottom ε_c^B of the section versus average curvature are represented. In these ranges, only the rebars react to the external bending moment since the concrete is completely damaged in tension. At the end of the unloading phase, plasticity occurs in the compressed concrete.

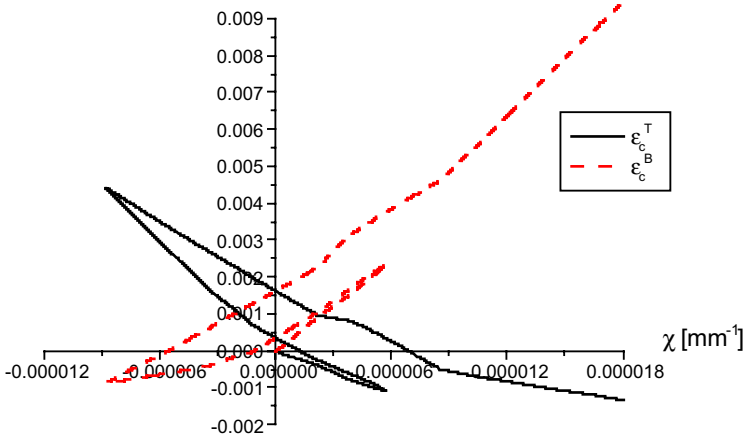

Fig. 14. Average strain in concrete at the top ε_c^T and at the bottom ε_c^B of the section versus average curvature.

Finally, in Fig. 15 the bond stress versus slip at the steel–concrete interface, evaluated near the cracked section, for the top and bottom reinforcements during the second examined cyclic loading is represented. It can be noted that during the reloading a degradation of the stiffness and of the maximum bond stress occur at the bottom reinforcements.

Also in these analyses the accuracy of the assumed value for the cracking distance 2λ has been verified computing the stress in the concrete at the section $z = 0$.

4.2. Comparisons with experimental results

The validation of the proposed model has been performed through a comparison with experimental data available in literature. In particular, the experimental cyclic bending behavior of a cantilever beam, presented in Kwak and Kim (2001), is simulated.

The following material properties are adopted:

- Concrete:

  $E_c = 25{,}310.4$ MPa $f_c = 25$ MPa $K_c = 3260$ MPa $\varepsilon_0^+ = 0.00014$ $\varepsilon_0^- = -0.0012$
  $\varepsilon_u^+ = 0.000286$ $\varepsilon_u^- = -0.0020$

- Steel:

  $E_s = 204{,}662.5$ MPa $\sigma_s = 460.5$ MPa $K_s = 0.0$ MPa $m_s = 6.5$ $\delta_{sat} = 135.0$ MPa
  $C_{start} = 610.0$ $C_{fin} = 100.0$ $a_{start} = 215.0$ MPa $a_{final} = 180.0$ MPa $C_{exp} = 50000.0$
  $a_{exp} = 50000.0$

- Steel–concrete interface:

  $K_\tau = 250$ N/mm^3 $\tau_1 = 10$ MPa $\tau_2 = 2.5$ MPa $s_1 = 0.1$ mm $s_2 = 2.0$ mm $s_3 = 3.5$ mm

The geometrical characteristics are set as:

$\lambda = 200$ mm $b = 228.6$ mm $h = 406.4$ mm $y_1 = -166.2$ mm $y_2 = 166.2$ mm

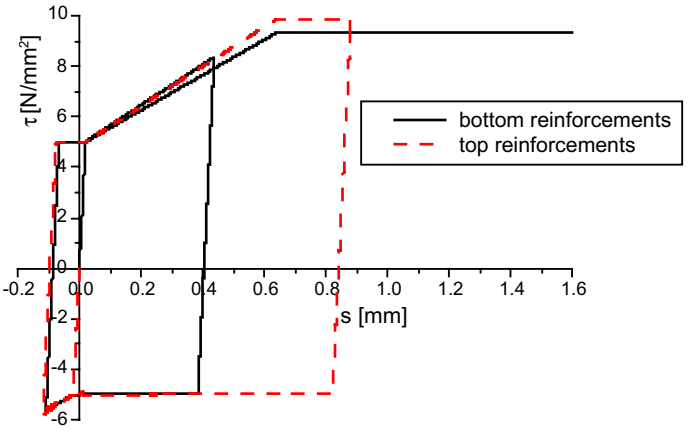

Fig. 15. Bond stress versus slip at the concrete–steel interfaces, close to the cracked section, during cycles for the top and bottom reinforcements.

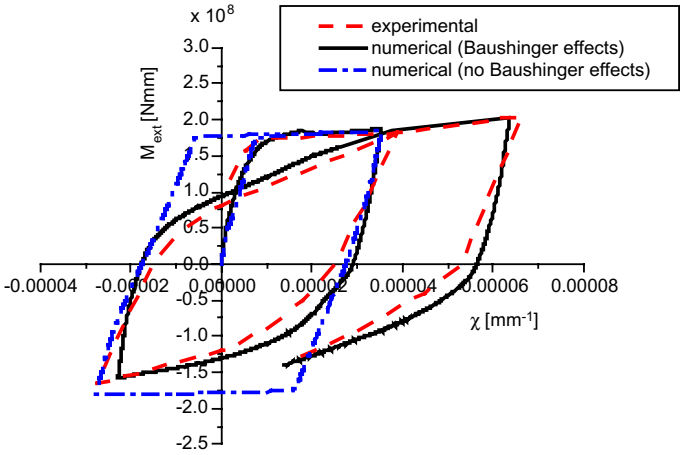

Fig. 16. Cyclic bending behavior: comparison between the numerical and experimental results.

Two numerical analyses are performed. In a first case only the linear isotropic hardening, with $K_s = 100$ MPa, is considered for the steel, while in the second case both the isotropic and kinematic hardening are accounted for, with the parameters reported above, in order to reproduce the Baushinger effect.

The obtained results, summarized by the relationship between the bending moment and the flexural curvature, are compared in Fig. 16 with the numerical outcomes reported in Kwak and Kim (2001).

During the first loading cycle both the models appear in good agreement with the experimental results and are able to simulate in a correct way the strength and stiffness of the specimen. The comparison can be considered satisfactory also in the first phase of the unloading branch. Nevertheless when the external moment becomes negative, during the unloading phase, the obtained results highlight the necessity to account for the Baushinger effect. In fact, when only isotropic hardening is considered for the steel, significant different behavior can be found with respect to experimental outcomes, particularly with reference to the stiffness of the element.

On the contrary, a satisfactory agreement is obtained when both the isotropic and kinematic hardening are considered. In this case the stiffness degradation is effectively simulated and the numerical results agree with the experimental ones also for the subsequent loading and unloading cycle.

The effectiveness of the model in reproducing the experimental response points out the necessity of considering the element behavior, rather than the cross-section behavior, and accounting for the cracking and slip phenomena. Furthermore, it appears important to consider the Baushinger effect in steel in cyclic analyses.

5. Conclusions

A one-dimensional model for a beam element of reinforced concrete is proposed. In particular, an elastoplastic-damage model is developed for the concrete material introducing two damage variables, one in tension and one in compression, accounting for the crack closure unilateral phenomenon. In particular, the damage evolution is governed by the elastic strain as the experimental evidences show. A plasticity model with nonlinear isotropic and kinematic hardening is adopted for the steel of the bars. Furthermore a bond stress–slip law is introduced for the steel–concrete interface. The model appears simple and effective. In fact, it is defined by a reduced number of parameters with a clear physical meaning.

The developed numerical procedure, based on the arc-length method, is able to determine the complex behavior of reinforced cementitiuous elements. The proper choice of the control parameters allows to follow the load-displacement equilibrium curve, characterized by softening branches.

The presented one-dimensional model and numerical procedure can be useful to derive fundamental considerations on the mechanical response of cementitious elements reinforced by classical steel bars. In fact, the damage and plastic effects, taken into account in the material constitutive law, significantly influence the beam element behavior. The proposed model highlights the cyclic behavior of reinforced concrete elements, and, in particular, it provides the stress and strain distributions along the rebars and at the interfaces, during the loading history. This last aspect could be of paramount importance in structures in seismic zone, whose mechanical response can be strongly affected by local brittle failure due to bond-slip behavior or by steel strain localization.

The results obtained by numerical applications clearly show the differences in structural behavior when considering the whole element rather then the classical single section. Through comparisons with experimental results available in literature, the following conclusions are obtained:

- The influence of the tension-stiffening effects, of the bond-slip behavior and of the steel strain localization in simple beam elements subjected both to monotonic and cyclic loads cannot be neglected, particularly in the evaluation of the local ductility.
- Proper simulation of the softening behavior of concrete in compression is necessary for predicting strength degradation; in particular, the effect of transversal reinforcement in reinforced concrete beams has to be taken into account, also in the simplified way proposed by Park and Paulay (1975).
- Proper definition of the crack distance is necessary, in order to evaluate the average behavior of the structural element.
- Uncertainties are still connected to the cyclic bond-slip law, particularly in the unloading branches.
- The Baushinger effect of the reinforcing steel can play a significant influence on the cyclic behavior and must be reproduced in a suitable way.

Finally, the proposed model can be effectively used to predict structural response under cyclic loading, and its application can be useful for the evaluation of the safety level of structures subjected to dynamic or cyclic loads.

References

Abu-Lebdeh, T.M., Voyiadjis, G.Z., 1993. Plasticity–damage model for concrete under cyclic multiaxial loading. J. Eng. Mech. 119 (7), 1465–1484.

Addessi, D., Marfia, S., Sacco, E., 2001. A plastic nonlocal damage model. Comput. Meth. Appl. Mech. Eng. 191, 1291–1310.

Ayoub, A., Filippou, F., 1999. Mixed formulation of bond-slip problems under cyclic loads. J. Struct. Eng. 125 (6), 661–671.

Balàzs, G.L., 1991. Fatigue of bond. ACI Mater. J. 88 (6), 620–629.

Bigaj, A.J., 1999. Structural Dependence of Rotation Capacity of Plastic Hinges in R.C. Beams and Slabs. Delft University of Technology, Delft University Press.

Borino, G., Fuschi, P., Polizzotto, C., 1996. Elastic–plastic–damage constitutive models with coupling internal variables. Mech. Res. Commun. 23 (1), 19–28.

Carol, I., Bažant, Z., 1997. Damage and plasticity in microplane theory. Int. J. Solids Struct. 34 (29), 3807–3835.

CEB-FIP Bulletin, 2000. Bond of reinforcement in concrete.

CEB-FIP, 1990. Model Code. Thomas Telford.

Chan, W.L., 1955. The ultimate strength and deformation of plastic hinges in concrete frameworks. Mag. Concr. Res. 7 (21), 121–132.

Ciampi, V., Eligehausen, R., Bertero, V.V., Popov, E.P., 1981. Analytical model for deformed-bar bond under generalized excitations. Trans. IABSE Colloquium on Advanced Mechanics of Reinforced Concrete, Delft, Netherlands.

Crisfield, M.A., 1991. Non-linear Finite Element Analysis of Solids and Structures, vol. 1. John Wiley & Sons Ltd., England.

de Borst, R., Pamin, J., Geers, M.G.D., 1999. On coupled gradient dependent plasticity and damage theories with a view to localization analysis. Eur. J. Mech. A/Solids 18, 939–962.

Eligehausen, R., Popov, E.P., Bertero, V.V., 1983. Local bond stress–slip relationship of deformed bars under generalized excitations. Report No. UCB/EERC 83-23, University of California, Berkeley.

EUROCODE 2, 1993. Design of concrete structures—UNI ENV 1992-1-1.

Filippou, F.C., Popov, E.P., Bertero, V.V., 1983. Modeling of reinforced concrete joints under cyclic excitations. ASCE, J. Struct. Eng. 109 (11), 2666–2684.

Gambarova, P.G., Rosati, G.P., 1996. Bond and splitting in reinforced concrete: test results on bar pull-out. Mater. Struct., RILEM 29, 267–276.

Grimaldi, A., Rinaldi Z., 2000. Influence of the steel properties on the ductility of r.c. structures. Proc. XII World Conference on Earthquake Engineering WCEE, Auckland, New Zealand.

Harajli, M.H., Hout, M., Jalkh, W., 1995. Local bond stress–slip behavior of reinforcing bars embedded in plain and fiber concrete. ACI Mater. J. 92 (4), 343–354.

Hillerborg, A., 1983. Analysis of one single crack. In: Wittmann, F.H. (Ed.), Fracture Mechanics of Concrete. Elsevier, pp. 223–249.

Kankam, C.K., 1997. Relationship of bond stress, steel stress and slip in reinforced concrete. J. Struct. Eng. 123 (1), 79–85.

Kent, D.C., Park, R., 1971. Flexural members with confined concrete. J. Struct. Div., ASCE 97 (ST7), 1969–1990.

Kwak, H.-G., Kim, S.-P., 2001. Non linear analysis of rc beams subjected to cyclic loading. J. Struct. Eng. 127 (12), 1436–1444.

Kwan, W.P., Billington, S.L., 2001. Simulation of structural concrete under cyclic load. J. Struct. Eng. 127 (12), 1391–1401.

Lee, J., Fenves, G.L., 1998. Plastic–damage model for cyclic loading of concrete structures. J. Eng. Mech. ASCE 124, 892–900.

Lemaitre, J., Chaboche, J.L., 1990. Mechanics of Solids Materials. University Press Cambridge.

Luccioni, B., Oller, S., Danesi, R., 1996. Coupled plastic-damaged model. Comput. Meth. Appl. Mech. Eng. 129, 81–89.

Markeset, G., 1993, Failure of concrete under compressive strain gradient. Ph.D. Thesis, The Norwegian Institute of Technology, Trondheim.

Monti, G., Spacone, E., 2000. Reinforced concrete fiber beam element with bond-slip. J. Struct. Eng. 126 (6), 654–661.

Morita, S., Kaku, T., 1973. Local bond stress–slip relationship under repeated loading. Proc. IABSE Simposyum: Resistance and Ultimate Deformability of Structures Acted on by Well Defined Repeated Loads, Lisboa, pp. 221–227.

Meschke, G., Lackner, R., Mang, H.A., 1998. An anisotropic elastoplastic–damage model for plain concrete. Int. J. Numer. Meth-Eng. 42, 703–727.

Ngo, D., Scordelis, A.C., 1967. Finite element analysis of reinforced concrete beams. ACI J. 64 (3), 152–163.

Park, R., Paulay, T., 1975. Reinforced Concrete Structures. John Wiley and Sons, New York.

Ramtani, S., Berthaud, Y., Mazars, J., 1992. Orthotropic behavior of concrete with directional aspects: modelling and experiments. Nucl. Eng. Des. 133, 97–111.

Rehm, G., 1961. On the fundamentals of steel–concrete bond (in German). Deutscher Ausschuss fur Stahlbeton (138), 1–59.

Sargin, M., Ghosh, S.K., Handa, V.K., 1971. Effects of lateral reinforcement upon the strength and deformation properties of concrete. Mag. Concr. Res. 23 (75–76), 99–110.

Simo, J.C., Hughes, T.J.R., 1998. Computational Inelasticity. Springer-Verlag, New York.

Soh, C.K., Chiew, S.P., Dong, Y.X., 1999. Damage model for concrete–steel interface. J. Eng. Mech. 125 (8), 979–983.

Tassios, T.P., Yannopoulos, P.J., 1981. Analytical studies on reinforced concrete members under cyclic loading based on bond stress–slip relationships. ACI J. 78 (3), 206–216.

Yoshida, F., Uemori, T., Fujiwara, K., 2002. Elastic–plastic behavior of steel sheets under in-plane cyclic tension–compression at large strain. Int. J. Plast. 18, 633–659.